

Density-functional theory of simple classical fluids. I. Surfaces*

C. Ebner

*Department of Physics, The Ohio State University, Columbus, Ohio 43210
and Battelle Memorial Institute, Columbus, Ohio 43201*

W. F. Saam

Department of Physics, The Ohio State University, Columbus, Ohio 43210

D. Stroud

*Department of Physics, The Ohio State University, Columbus, Ohio 43210
and Battelle Memorial Institute, Columbus, Ohio 43201*

(Received 27 May 1976)

A density-functional theory appropriate to nonuniform simple classical fluids is developed. Unlike most previous theories, the theory is in principle exact in the linear-response regime. For practical applications a small number of well-defined approximations, including that of Percus and Yevick, are made. Given only the Lennard-Jones 6-12 potential as input, the theory yields surface tensions and profiles in very good agreement with the results of Monte Carlo calculations. For a liquid pressed against a hard wall the expected oscillations in density in the vicinity of the wall are obtained. Comparisons with previous theories are made, and points of possible improvement in the formalism are discussed.

I. INTRODUCTION

The physics of nonuniform many-body systems has developed rapidly in recent years. The most-studied type of nonuniformity is, of course, a surface. The situation regarding metal surfaces, for which density-functional (DF) theory is reasonably highly developed, is reviewed by Lang.¹ Liquid-surface physics prior to 1973 is reviewed by Croxton²; more recent work in this area will be discussed below. Low-energy-electron-diffraction (LEED) techniques have produced important advances in solid-state surface physics.³ A new theory of the free surface of zero-temperature ⁴He is given in a recent paper by two of us.⁴ This paper reviews earlier work.

Extant theoretical work relies heavily on the large body of previous results for uniform systems. In particular, local free energies and two-particle correlation functions from uniform-system theories are used in describing nonuniform systems. It is our position that this procedure should involve minimal use of disparate approximations within the uniform-system physics in order that new effects due to nonuniformities be most easily understood. Density-functional theory is ideal from this point of view. Most previous theories of surfaces of classical liquids are not. In this paper we develop and solve a DF theory of classical liquid surfaces. The theory is conceptually simple, contains as few independent approximations as appears presently feasible, and is solved without resorting to such simplifications as gradient expansions, an approach which turns an intrinsically

nonlocal problem into a local one. Our results are in good agreement with the appropriate available data. Further, we are able to clearly identify specific aspects of the theory where approximations can in principle be eliminated and to assess the amount of numerical work needed to implement these improvements.

The theory which we use is the classical version of the recent DF theory for liquid ⁴He referred to above.⁴ It requires as input the direct correlation function $c(n, T)$ of a uniform system as a function of number density n and temperature T , as well as the local free-energy density $f(n, T)$. The latter, of course, may be obtained from the former in various ways, e.g., by means of the compressibility sum rule. The formalism correctly reproduces linear-response theory. In order to test this theory, we apply it to a fluid characterized by Lennard-Jones 6-12 interactions, obtaining the required $c(r; n, T)$ from the Percus-Yevick (PY) approximation.⁵ We also briefly consider some simpler methods of determining f and c . The theory is developed in Sec. II, where its major overall features are compared with those of the very recent work of Bongiorno and Davis⁶ and the slightly older results of Toxvaerd.^{7,8}

Section III provides the details of the calculations of $c(r; n, T)$, the free energy, and the phase diagram for a 6-12 fluid. Solutions of the PY equation much more extensive than any previous ones are obtained. Tables of the pair correlation functions $g(r; n, T)$ have been placed in a document repository.⁹ The contents of the tables are described in Sec. III.

In Sec. IV the surface tension and detailed surface density profiles are computed. Good agreement with a variety of Monte Carlo calculations¹⁰⁻¹⁴ is obtained. As discussed by Lee, Barker and Pound,¹⁰ agreement between the theoretical surface tension and that measured for real argon to within ~20% requires the inclusion of three-body forces. An interesting check of our theory is also carried out in Sec. IV. On the basis of an obvious analogy with the pair correlation function, one would expect that the liquid density should oscillate in the vicinity of the interface between a hard wall and the liquid. For the case of a semihard wall constructed by summing a $1/r^{12}$ repulsive pair potential over uniformly distributed atoms, yielding a $1/z^9$ (z is the coordinate normal to the interface, measured from the interface) potential, we do find such behavior. Quite substantial oscillations are obtained. A simplified version of our theory, having the twin virtues that all required input exists in analytic form and that the predictions differ little from our more elaborate theory, is briefly presented in Sec. V.

A critical discussion of the results, including areas where approximations might be improved, is given in Sec. VI.

II. FORMALISM

The essential entity in our theory is the Helmholtz free energy of the system $F[n]$ expressed as a *functional* of the particle number density $n(\vec{r})$ at point \vec{r} . Following ideas of Hohenberg and Kohn¹⁵ for the $T=0$ case, Mermin¹⁶ showed that given $F[n]$, the density is determined by minimizing the quantity

$$\Omega = F[n] + \int d^3r n(\vec{r}) [v(\vec{r}) - \mu] \quad (2.1)$$

at constant temperature T , external potential $v(\vec{r})$, and chemical potential μ . The minimization is achieved by varying $n(\vec{r})$, the result being that $n(\vec{r})$ is the solution to the functional equation

$$\delta F[n] / \delta n(\vec{r}) = \mu - v(\vec{r}). \quad (2.2)$$

In practice, of course, an approximate rather than exact form must be used for $F[n]$. An extension of the arguments⁴ for the case of $T=0$ liquid ⁴He yields the approximation

$$F[n] = \int d^3r f(n(\vec{r})) - \frac{1}{4} \int d^3r d^3r' K(\vec{r} - \vec{r}'; \bar{n}) \times [n(\vec{r}) - n(\vec{r}')]^2, \quad (2.3)$$

where $f(n)$ is the free-energy density of the uniform system at density n , and

$$K(\vec{r} - \vec{r}'; n) = \int \frac{d^3q}{(2\pi)^3} \frac{e^{i\vec{q} \cdot (\vec{r} - \vec{r}')}}{\chi_q(n)} \quad (2.4)$$

is the Fourier transform of the inverse of the retarded density-density response function¹⁷ of a uniform system at density n . The average density appearing in (2.3) may be chosen in various ways. One convenient and intuitively appealing choice of the \bar{n} is

$$\bar{n} = \frac{1}{2} [n(\vec{r}) + n(\vec{r}')] . \quad (2.5)$$

Other nonlocal averages are discussed later on. Equations (2.3)–(2.5) are exact for the situation where the density varies only slightly from a uniform, constant average, i.e., in the linear response regime. Away from this regime the theory assumes simply that the physics underlying $F[n]$ can be described in terms of a local free energy $f(n(\vec{r}))$ plus a nonlocal effective interaction between parts of the system at \vec{r} and \vec{r}' . The nonlocal interaction is related to the density response function, and corrections to linear-response theory are assumed to be accounted for by use of a nonlocal average density \bar{n} .

For a single-component classical liquid

$$\chi_q^{-1}(n) = (k_B T/n) [1 - nc_q(n)] , \quad (2.6)$$

where $c_q(n)$ is the Fourier transform of the direct correlation function $c(r; n)$ at wave number q , and k_B is Boltzmann's constant. Combination of (2.3)–(2.6) yields immediately

$$F[n] = \int d^3r f(n(\vec{r})) + \frac{k_B T}{4} \int d^3r d^3r' c(\vec{r} - \vec{r}'; \bar{n}) \times [n(\vec{r}) - n(\vec{r}')]^2. \quad (2.7)$$

Our theory of nonuniform classical systems is thus specified by (2.2), (2.7), and a prescription for obtaining $c(r; n)$ and $f(n)$ [$f(n)$ is derivable from $c(r; n)$] from a microscopic theory of the uniform fluid. The prescription we choose¹⁸ is that of Percus and Yevick (PY),¹⁹ which is both widely used and reasonably accurate.²⁰ Details of the PY calculation are given in Sec. III; the pair potential chosen is a Lennard-Jones 6-12 potential.

It is appropriate at this point to compare the formal basis of our theory with other theories of nonuniform classical fluids. All theories involve approximations, and the extent to which these approximations can be understood and controlled becomes an important point, especially when the gross features and some of the results of the theories, such as their predictions of surface tensions, are quite similar.

The most recent theory, and perhaps the most similar to ours in spirit, is that due to Bongiorno and Davis.⁶ These authors do in fact obtain and minimize a free-energy functional in order to obtain the surface tension and density profile. However, in their theory the local and nonlocal parts

of their functional come from *different* approximate theories; the nonlocal part is incorrect in the regime where linear-response theory holds; and the nonlocal part is approximated by a gradient expansion cut off at second order, in order to simplify the computations. Our work suffers from none of these defects. Further, second-order gradient expansions cannot yield density oscillations of the sort expected in a liquid in the vicinity of a hard wall; our formalism predicts oscillations (see Sec. IV). Other recent work is due to Toxvaerd. He has two approaches, which we label T1 and T2.⁸ In T1 a free-energy functional is minimized. However, the functional is constructed from a somewhat bewildering array of unrelated approximations, and, like that of Bongiorno and Davis, fails to reproduce linear-response theory. An application of T1 is given in Ref. 7. In T2 a BGYB integral equation is solved for the particle number density in the surface region, given a simple approximation for the pair correlation function in terms of the actual density and the pair correlation functions in the liquid and the gas phase. The theory is clean and the approximations are clear, as is the case with our theory. Its very nature is, however, much different from theories based on a free-energy minimization scheme. Comparisons of results from such different approaches with both experiments on real argon and with computer "experiments" are quite valuable insofar as neither approach yet represents a truly controlled approximation scheme. Further work along both avenues is desired, and some suggestions are put forth in Sec. VI.

III. NUMERICAL RESULTS FOR THE UNIFORM SYSTEM

In this section we first describe our method of finding solutions to the Percus-Yevick equation. This is followed by the determination of the thermodynamic functions in the uniform system, from which the vapor-liquid phase diagram is obtained.

The Percus-Yevick equation is¹⁹

$$c(r) = g(r)(1 - e^{\beta V(r)}); \quad (3.1)$$

$c(r)$ and $g(r)$ are, respectively, the direct and pair correlation functions, $V(r)$ is the interatomic potential, and $\beta = 1/k_B T$. The potential is taken to be the Lennard-Jones (6-12) interaction,

$$V(r) = 4\epsilon[(\sigma/r)^{12} - (\sigma/r)^6]. \quad (3.2)$$

In applying the results to the particular case of liquid argon we have set $\epsilon/k_B = 119.8$ K and $\sigma = 3.405$ Å.²¹

A second equation relating $c(r)$ and $g(r)$ is the defining relation²⁰

$$g(r) - 1 = c(r) + n \int d^3 r' [g(|\vec{r} - \vec{r}'|) - 1]c(r'), \quad (3.3)$$

where n is the particle number density.

Equations (3.1) and (3.3) may be combined to find a nonlinear integral equation for either $c(r)$ or $g(r)$. The equation for $c(r)$ is

$$c(r) = e^{-\beta V(r)} - 1 - n \int_0^\infty dr' Q(r, r')c(r'), \quad (3.4)$$

where

$$Q(r, r') = 2\pi(1 - e^{-\beta V(r)}) \frac{r'}{r} \times \int_{|r'-r|}^{|r'+r|} y dy \left(\frac{c(y)}{1 - e^{-\beta V(y)}} - 1 \right). \quad (3.5)$$

We have solved (3.4) using the following procedure: A guess is made of the function $c(r)$ and this function is used to evaluate $Q(r, r')$ and the right-hand side of (3.4). The left-hand side is then a predicted $c(r)$ which may in turn be used to make a second prediction, and so on. In practice it turns out to be necessary to use a linear combination of the predicted $c(r)$ and the previous one in order that this iterative process converge. We repeated the procedure until two successive functions $(r/\sigma)g(r)$ agreed to 1 part in 10^5 for all values of r ; this criterion is the same as that of Throop and Bearman²² and gives convergence of the pair correlation function to within 0.0001.

There are two other sources of numerical error in solving (3.4). One is the necessity of truncating the integration over y in (3.5) at that largest value of y for which $c(y)$ has been obtained from (3.4). We employed 8σ as the maximum value of r and r' in (3.4) and simply set $g(y) = 1$ in (3.5) for $y > 8\sigma$. This approximation was checked by extending r and r' to 10σ in some cases. The error produced in $g(r)$ by truncating at 8σ is generally no larger than 0.0001 and usually smaller. There are exceptions, first, for n and T close to the spinodal line and, second, for n large (the largest n considered is $n = 1/\sigma^3$). Of the first category an example is at $n^* \equiv n\sigma^3 = 0.25$ and $T^* \equiv T/\epsilon = 1.4$; then $g(r)$ has a long, slowly convergent tail which is ~ 1.001 even at $v = 8\sigma$. The truncation at $r/\sigma = 8$ results in a maximum error in $g(r)$ of 0.0006 both around the peak in the pair correlation and at $r \sim 8\sigma$. At other values of r the error is of order 0.0001. As for the functions at $n^* = 1.0$, the solution for $g(r) - 1$ has an oscillatory long-range behavior such that the amplitude of the oscillations at $r = 8\sigma$ is still ~ 0.002 . The truncation at $r = 8\sigma$ produces a maximum error in $g(r)$ of about 0.0015.

The final source of error lies in the numerical formula used to perform the integrals over r' and y in (3.4) and (3.5). We employed Simpson's rule

throughout with a step size $\delta r = 0.025\sigma$. A check on this procedure was obtained by also using $\delta r = 0.0125\sigma$ in some cases. The error in $g(r)$ turns out to generally be much smaller than 0.0001 except at $n^* = 1.0$, where it can be as large as 0.0004 around the first peak in the pair correlation function.

As an additional check on our work, we have compared our computed pair correlation functions with the ones found by Throop and Bearman (TB) at those values of n and T which are common to both our work and that of TB. For those functions which have converged to within 0.0002 of unity at $r = 6\sigma$, the agreement is generally within 0.0002 for all r ; an example is $g(r)$ at $n^* = 0.5$ and $T^* = 1.4$. In those cases where $g(r)$ still differs appreciably from 1 at 6σ , however, there are considerably larger discrepancies. An example is $T^* = 1.4$ and $n^* = 0.25$, where $g(r = 6\sigma) \approx 1.004$; our correlation function in this case differs from that in Ref. 18 by as much as 0.002. In such cases our solutions are undoubtedly the more accurate ones.

In Ref. 9 one may find tables of the solutions $g(r; n, T)$ at 76 points in the nT plane; the locations of these points are given by the x 's in Fig. 1. Each function is expressed to four figures beyond the decimal point and is tabulated at intervals in r/σ of 0.025 for $0.875 \leq r/\sigma \leq 8.0$; for $r/\sigma < 0.875$, the pair correlation function is zero to the same number of digits.

Much has been written concerning the solutions to the Percus-Yevick equation²²⁻²⁸ and we see no point in adding to this voluminous literature here. Rather, we shall merely point out that they, at the

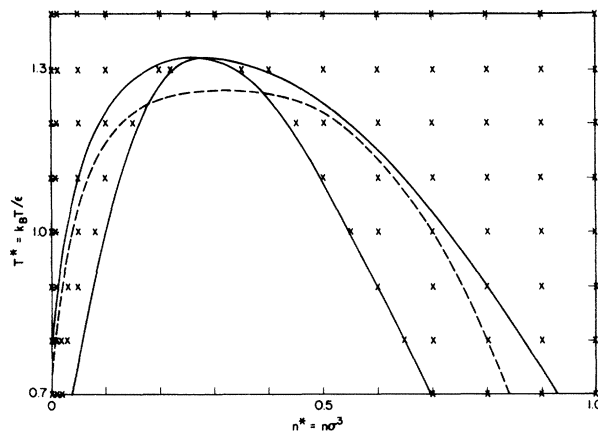


FIG. 1. Phase curves in the $T^* - n^*$ plane. The inner solid curve is the spinodal curve calculated using the Percus-Yevick (PY) theory. The outer solid curve is the coexistence curve resulting from the PY theory. The x 's are points at which the Percus-Yevick equation was solved. The dashed line is the experimental coexistence curve for argon (Ref. 29).

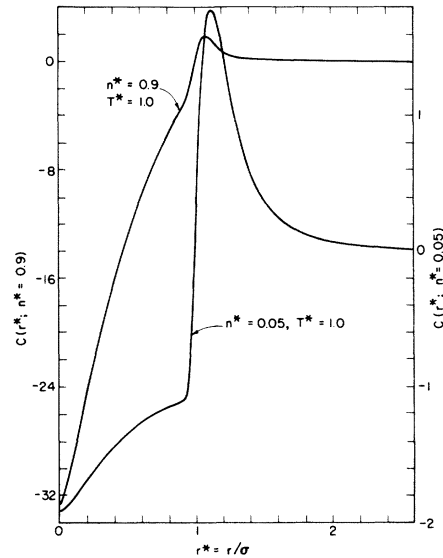


FIG. 2. Direct correlation function $c(r^*, n^*, T^*)$ obtained from the Percus-Yevick theory. Plots are given for $c(r^*, n^*, T^*)$ vs r^* for the cases $n^* = 0.05$, $T^* = 1.0$, and $n^* = 0.9$, $T^* = 1.0$.

very least, possess all of the qualitative physical features of $c(r)$ and $g(r)$ in the vapor and liquid regimes. This fact is nicely demonstrated in Figs. 2 and 3; Fig. 2 shows $c(r, n^* = 0.05, T^* = 1.0)$ and $c(r, n^* = 0.9, T^* = 1.0)$ where $T^* \equiv kT/\epsilon$ and $n^* = n\sigma^3$. The former case is in the vapor phase and the latter in the liquid phase. Figure 3 shows the pair

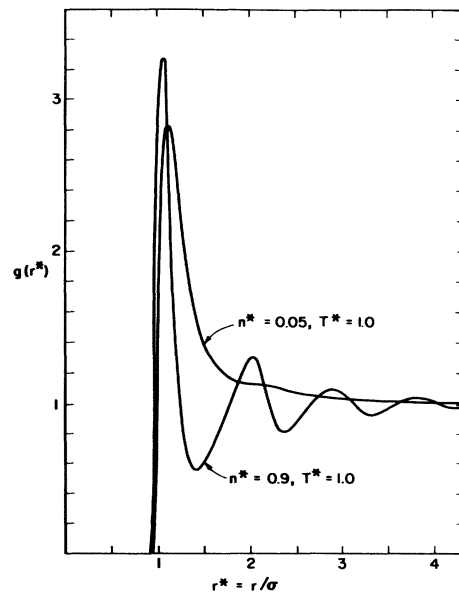


FIG. 3. Pair-correlation function $g(r^*, n^*, T^*)$ obtained from the Percus-Yevick theory. Plots are given of $g(r^*, n^*, T^*)$ vs r^* for the cases $n^* = 0.05$, $T^* = 1.0$ and $n^* = 0.9$, $T^* = 1.0$.

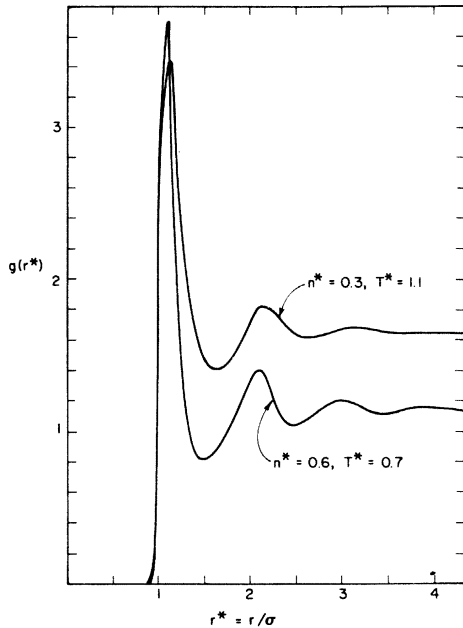


FIG. 4. Pair-correlation functions $g(r^*, n^*, T^*)$ obtained from the Percus-Yevick theory for values of n^* , T^* in the unstable (spinodal) region. Shown are the cases $n^* = 0.3$, $T^* = 1.1$, and $n^* = 0.6$, $T^* = 0.7$.

correlation functions at the same densities and temperature.

For all of the correlation functions tabulated,⁹ $nc_{\bar{q}=0} \equiv n \int d^3r c(r) < 1$. If $nc_{\bar{q}=0} > 1$, the uniform system is mechanically unstable since

$$\left(\frac{\partial P}{\partial n}\right)_T = kT[1 - nc_{\bar{q}=0}(n, T)] < 0. \quad (3.6)$$

There is a large portion of the $n - T$ plane where this inequality is satisfied and, within this region, the Percus-Yevick equation does not have any physically reasonable solutions. We have succeeded in finding numerical solutions of (3.4) in this region, but they have a distinctly unphysical behavior in that $g(r)$ approaches a value different from unity at large r . As examples we show $g(r, n^* = 0.3, T^* = 1.1)$ and $g(r, n^* = 0.6, T^* = 0.7)$ in Fig. 4.

In applying the density-functional formalism to a case where the local density can be in the forbidden part of the two-phase region (e.g., near a free surface), we require direct correlation functions in this region but do not wish to use the PY solutions because of their unphysical form. Instead we have constructed an extrapolation and interpolation procedure in the $n - T$ plane to continue the PY solutions for $c(r, n, T)$ outside of the mechanically unstable region into this region. The direct correlation functions constructed in this way are thus *not* solutions of the Percus-Yevick equation in the un-

stable region but they do have physically reasonable behavior and join smoothly onto the PY solutions outside the unstable region. A number of different extrapolation and interpolation formulas of varying degrees of complexity were investigated before we settled on the following, relatively simple one:

$$c(r, n, T) = c(r, n, T_0) \left[\left(\frac{n - n_v}{n_l - n_v} \right) \left(\frac{c(r, n_l, T)}{c(r, n_l, T_0)} \right) + \left(\frac{n_l - n}{n_l - n_v} \right) \left(\frac{c(r, n_v, T)}{c(r, n_v, T_0)} \right) \right], \quad (3.7)$$

where n_l and n_v are densities in the liquid and vapor regions outside of the unstable region for all T under consideration. We chose $n_l^* = 0.7$ and $n_v^* = 0.01$. For any given n , T_0 was taken to be the smallest temperature for which we have a solution to the PY equation.

Other relations than (3.7) of course do not produce the same correlation functions. However, we generally found that more complicated extrapolations in temperature or more elaborate interpolations in n changed $c(r, n, T)$ by no more than a few per cent even as did other choices of n_l , n_v , and T_0 . Such uncertainties in the direct correlation function have an effect of order 1% on the properties of the nonuniform system examined in Sec. IV. Hence we feel the functions determined by (3.7) are quite adequate for our purposes.

Given the $c(r, n, T)$, we may find the pressure by integrating (3.6) over the density; the chemical potential is similarly found by integrating

$$\left(\frac{\partial \mu}{\partial n}\right)_T = \frac{kT}{n} [1 - nc_{\bar{q}=0}(n, T)]. \quad (3.8)$$

Next, making use of the fact that the grand canonical free-energy density $\omega(n, T)$ is just $-P$, we easily find the Helmholtz free-energy density,

$$f(n, T) = \omega(n, T) + n\mu(n, T) = -P(n, T) + n\mu(n, T). \quad (3.9)$$

In Fig. 5 we show the Helmholtz free-energy density in units of ϵ/σ^3 for $T^* = 0.7, 1.0$, and 1.3 .

Finally, we wish to consider the vapor-liquid phase diagram in the $n - T$ plane. At a given T , the vapor and liquid equilibrium densities may be found by making the standard common tangent construction on, e.g., the curves in Fig. 5; these densities are determined by the criteria that the chemical potentials and the pressures be the same in both phases:

$$P(n_v, T) = P(n_l, T), \quad \mu(n_v, T) = \mu(n_l, T). \quad (3.10)$$

The calculated coexistence curve is shown in Fig.

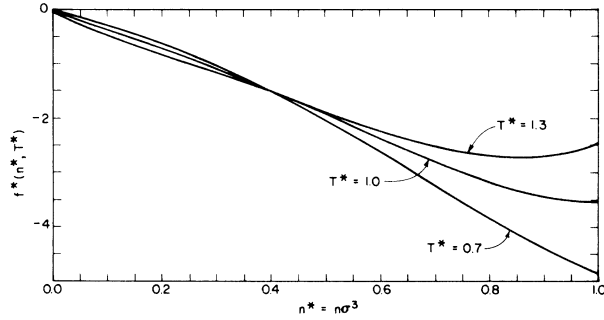


FIG. 5. Reduced Helmholtz free energy $f^*(n^*, T^*)$ calculated from the PY theory and plotted vs n^* for the cases $T^* = 0.7, 1.0, \text{ and } 1.3$.

1 along with the experimental one for argon.²⁹ Also shown is the calculated spinodal curve marking the points of instability of the liquid and vapor phases; $nc_{\bar{q}=0}(n, T) = 1$ defines the spinodal curve.

IV. SURFACE TENSION AND HARD WALL-LIQUID INTERFACE

The surface tension is found by calculating the free energy of a liquid-vapor system with a planar interface. Let the z axis be normal to the surface; then $n(\bar{r})$ is just $n(z)$ and (2.7) becomes

$$\mathcal{F}[n] = \int_{-\infty}^{\infty} dz f(n(z)) + \frac{kT}{4} \int_{-\infty}^{\infty} dz dz' K(z-z'; \bar{n}) \times [n(z) - n(z')]^2, \quad (4.1)$$

where

$$K(x; n) = \pi \int_0^{\infty} dy c((y+x^2)^{1/2}; n). \quad (4.2)$$

Also $\mathcal{F}[n]$ is the Helmholtz free energy of the system per unit area. At constant T and μ , it is the grand canonical free energy per unit area which is minimized, so we seek that density profile $n(z)$ which minimizes

$$\mathcal{Q}[n] = \mathcal{F}[n] - \mu \int_{-\infty}^{\infty} dz n(z) \quad (4.3)$$

and which also has the following properties:

$$\lim_{z \rightarrow \infty} n(z) = n_l(T), \quad (4.4)$$

$$\lim_{z \rightarrow -\infty} n(z) = n_v(T), \quad (4.5)$$

where $n_l(T)$ and $n_v(T)$ are the equilibrium liquid and vapor densities at temperature T .

The surface tension $\tau(T)$ is the difference between $\mathcal{Q}[n]$ and the grand canonical free energy per unit area if the system were composed simply of bulk liquid and bulk vapor:

$$\tau(T) = \int_{-\infty}^{\infty} dz [f(n(z)) - \mu n(z) + P] + \frac{k_B T}{4} \int_{-\infty}^{\infty} dz dz' K(z-z'; n) [n(z) - n(z')]^2. \quad (4.6)$$

At this point the task one faces is to find that $n(z)$ which minimizes $\tau(T)$, subject to the conditions (4.4) and (4.5). We have done this using a parametrized trial function for $n(z)$, minimizing $\tau(T)$ with respect to variation of the parameters. Several different functions were investigated using as many as six parameters. These functions were sufficiently flexible that $n(z)$ could exhibit either monotonic or oscillatory behavior. After some experimentation with the various functions we chose the following one for the most extensive calculations:

$$n(z) = n_v + (n_l - n_v)(1 + e^{-\alpha z})^{-1} \times \left[1 + \left(\sum_{p=0}^3 \gamma_p z^p \right) e^{-\beta z^2} \right], \quad (4.7)$$

where α , β , and the four γ_p 's are variational parameters.

As for the manner in which \bar{n} in (4.6) was chosen, we investigated the geometric mean $\bar{n} = [n(z)n(z')]^{1/2}$, the arithmetic mean $\bar{n} = \frac{1}{2}[n(z) + n(z')]$, and also used the density at the mean position, $\bar{n} = n[\frac{1}{2}(z + z')]$. The second and third choices led to very nearly identical results for $\tau(T)$ and for $n(z)$ while the geometric mean produced surface tensions that were slightly larger than those found by the other two methods. The maximum difference between surface tensions as calculated by the three \bar{n} 's was 6% at $T^* = 0.7$, and for $T^* > 0.9$ the difference was always less than 1%. The numerical results reported here were found using $\bar{n} = \frac{1}{2}[n(z) + n(z')]$; this is the same prescription for \bar{n} which we used in our earlier work on helium.

The calculated surface tension is exhibited in Fig. 6 in units of ϵ/σ^2 ; also given are the surface tension (experimental) of argon as well as the results of Monte Carlo calculations¹⁰⁻¹⁴ using a Lennard-Jones (6-12) potential between pairs of atoms. That the differences between the theoretical results for the (6-12) potential and the experimental data is due to the effects of three-body forces is fairly convincingly demonstrated by Lee, Barker, and Pound.¹⁰ The two-body Monte Carlo computations using the (6-12) potential and our calculation are in close agreement, a fact which we regard as strong evidence for the reliability of our density-functional formalism.

In Fig. 7 we show the surface density profiles $n^*(z)$ at $T^* = 0.7, 1.0, \text{ and } 1.2$. The agreement with the Monte Carlo profiles given in Refs. 10-13 is

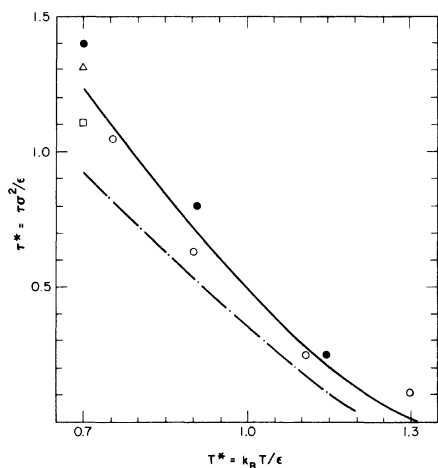


FIG. 6. Surface tension in units of ϵ/σ^2 vs $T^* = k_B T / \epsilon$. The solid curve is the result of our full density-functional theory for the Lennard-Jones (6-12) potential. The various points are the results of the computer simulations of Liu (Ref. 13) (\circ), Lee *et al.* (\square), Chapela *et al.* (Ref. 12) (\bullet), and Miyazaki *et al.* (Ref. 14) (Δ). The dot-dashed curve is the experimental one for argon (Ref. 29).

most satisfactory. The profile in every case is a monotonic function of z whose width increases with temperature; $n(z)$ is smooth with a rather larger healing length going into the liquid than going into the vapor.

As an interesting contrast we have also considered the density profile and interface energy at a repulsive wall. The potential is determined according to the scheme described in Sec. I. Assuming n_0 atoms per unit volume in the wall which occupies the half-space $z < 0$ and an interaction $4\epsilon_0(\sigma_0/r)^{12}$ between a wall atom and an argon atom, we find that the latter feels the potential

$$V(z) = \frac{4}{45} \epsilon_0 n_0 \sigma_0^3 (\sigma_0/z)^9 \quad (4.8)$$

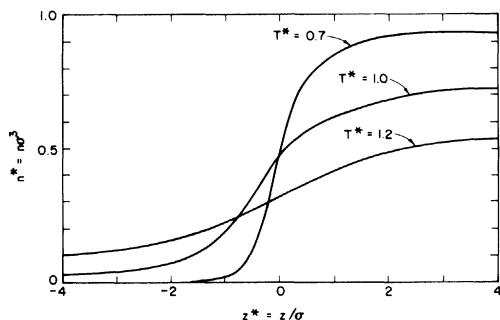


FIG. 7. Surface density profiles from the full density-functional theory. Shown are $n^*(z^*)$ vs z^* curves for $T^* = 0.7, 1.0,$ and 1.2 .

as a consequence of the existence of the wall. Thus the term

$$\epsilon_w[n] = \int_{-\infty}^{\infty} dz V(z)n(z)$$

should be added to the free energy. Thereafter the calculation becomes identical to the one just described for the surface tension except that $n(z)$ must go rapidly to zero as z approaches zero from positive values. Also, it is not necessary to pick (n_l, T) on the phase equilibrium boundary; rather we may pick any (n_l, T) at which the liquid (or the vapor, for that matter) is stable.

The trial density profile we have chosen in the form

$$n(z) = n_l e^{-\alpha/z^9} \left(1 + \sum_{p=0}^3 \gamma_p z^p e^{-\beta z^2} \right) (1 + e^{-\delta z})^{-1}$$

again after some experimentation. Here, $\alpha, \beta, \delta,$ and the γ_p are the variational parameters.

In Fig. 8 we show $n^*(z)$ for the case of $T^* = 1.1$ and $n^* = 0.73$. This result is typical. The profile has a maximum in the vicinity of $z = 0.75\sigma$, the height of the peak being an increasing function of n_l^* and rather insensitive to changes in T^* . There follows a minimum where the density falls some 40% below n_l^* . In some computer runs, this dip was followed by a second, smaller peak with a maximum height no more than 4% larger than n_l^* .

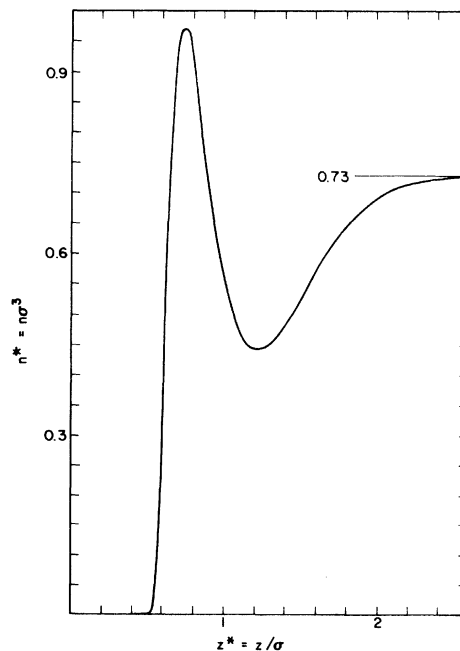


FIG. 8. Calculated liquid density profile $n^*(z^*)$ near a hard wall (potential $\sim 1/z^9$). The case $T^* = 1.1,$ $n^*(\infty) = 0.73$ is shown.

Because of the restrictions imposed on $n^*(z)$ by our choice of trial function, we are at present unable to say whether this second peak is really present; in any event, it is not large.

This oscillatory profile at a purely repulsive wall is qualitatively similar to the one that has been predicted⁴ to exist in liquid helium under similar circumstances. The fact that such behavior can emerge from our DF theory demonstrates, once again, its power and versatility.

V. SIMPLIFIED ANALYTIC APPROACH

The calculations described in the preceding sections are based on an exact numerical solution of the PY integral equation for a Lennard-Jones potential and are therefore highly accurate in principle. On the other hand, these calculations require considerable labor, in particular, a separate solution of the PY equation for each density and temperature of interest. It may, therefore, be useful to have available a simpler model, which, though perhaps less accurate, requires less computation. In this section, we describe one possible approach of this kind, and use it to compute the liquid-gas phase boundary and the surface tension of a Lennard-Jones fluid.

To find the free-energy density $f(n, T)$, we have used a variational principle based on the Gibbs-Bogolyubov inequality. For present purposes, this inequality takes the form³⁰

$$F \leq F_0 + \langle V \rangle_0, \quad (5.1)$$

where F is the Helmholtz free energy of the fluid (at fixed n and T), F_0 is the free energy of a reference fluid (at the same n and T) consisting of hard spheres of diameter d , and $\langle V \rangle_0$ is the pairwise interaction energy, calculated using the actual (Lennard-Jones) interactions and hard-sphere $g(r)$'s.

The variational principle consists of (i) minimizing the right-hand side of (5.1) with respect to d , and (ii) taking the resulting lowest upper bound to approximate F . This procedure has been successfully used in the past to treat the thermodynamics of both insulating and metallic fluids.³¹ In the case at hand, F_0 is available analytically within the PY approximation, while $\langle V \rangle_0$ has been evaluated for various values of d as a power series in $n^* = n\sigma^3$ by Rasaiah and Stell.³² If $F_0 + \langle V \rangle_0$, as evaluated in this way, is minimized with respect to d , then, as noted previously by Rasaiah and Stell, the resulting d/σ deviates from unity by less than 5% over the entire density and temperature range spanned by the liquid-gas coexistence curve. We have therefore simply taken $d = \sigma$. This gives the following analytic expression for $f^*(n^*)$:

$$\begin{aligned} T^{*-1}f^*(n^*) = & -\frac{3}{2}n^* + \frac{3}{2}n^*(1 - \frac{1}{6}\pi n^*)^{-2} \\ & - n^* \ln(1 - \frac{1}{6}\pi n^*) \\ & + (2\pi n^{*2}/T^*)(-0.9021 - 0.3321n^* \\ & - 0.2052n^{*2} + 0.3558n^{*3}), \end{aligned} \quad (5.2)$$

where $n^* = n\sigma^3$, $T^* = k_B T/\epsilon$, and $f^*(n^*) = n^*F$.

To complete the prescription for $F[n(r)]$, we have evaluated the correlation function $c(r; n, T)$ as

$$c(r; n, T) = c_{hc}(r; n) + \delta c_1(r; T) + \delta c_2(r; n, T). \quad (5.3)$$

$c_{hc}(r; n)$ is the direct correlation function for a liquid of number density n composed of hard spheres of diameter σ , evaluated in the PY approximation. $\delta c_1(r, T)$ is the contribution of the attractive tail of the Lennard-Jones potential, which we have approximated by

$$\begin{aligned} \delta c_1(r, T) = & e^{-V(r)/k_B T} - 1, \quad r > \sigma, \\ = & 0, \quad r < \sigma. \end{aligned} \quad (5.4)$$

$\delta c_2(r; n, T)$ is an additional correction to insure that c , when used in conjunction with (5.2), satisfies the compressibility sum rule. We have chosen δc_2 to be a step function of the form

$$\begin{aligned} \delta c_2 = & -\Delta(n, T), \quad r < \sigma, \\ = & 0, \quad r > \sigma. \end{aligned} \quad (5.5)$$

Note that the choice (5.4) for the tail contribution becomes exact in the limit of large r or small n . In order that this correct limiting behavior remain undisturbed, it seems desirable to require δc_2 to vanish for $r > \sigma$. The correction (5.5) is otherwise arbitrary but we have found that the surface ten-

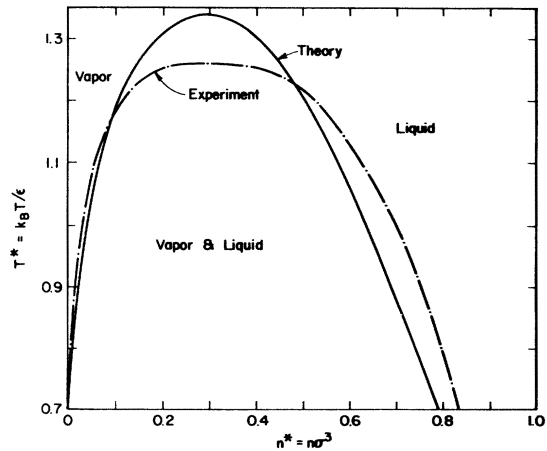


FIG. 9. Solid curve is the theoretical coexistence curve for a Lennard-Jones 6-12 fluid resulting from the simplified theory of Sec. V. The dot-dashed curve is the experimental coexistence curve for argon.

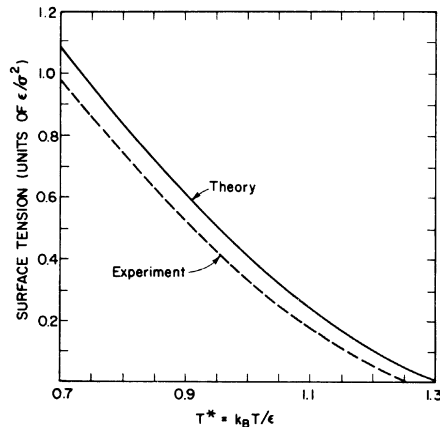


FIG. 10. Surface tension in units of ϵ/σ^2 vs $T^* = k_B T/\epsilon$. Shown are the results of the simplified theory of Sec. V (solid curve) and the experimental results (Ref. 29) for liquid argon (dashed curve).

sion is little altered when other plausible choices of δc_2 are used in place of (5.5); the phase diagram is, of course, unaffected.

The phase diagram and surface tension resulting from this simplified approach are shown in Figs. 9 and 10. The results are in fair accord with the Monte Carlo data¹⁰⁻¹⁴ and with experiments on argon, and are not greatly inferior to those of Secs. III and IV. Our conclusion is that the density functional approach to classical fluids, as described in Sec. II, can be used in conjunction with relatively simple forms for $c(r)$ and $f(n)$, such as, but not limited to, the forms described in this section. Such simpler forms could be useful in applying the DF approach to liquids with other than Lennard-Jones interactions, or extending it to mixtures.

VI. DISCUSSION

In this paper we have developed and applied a density-functional theory for nonuniform classical fluids. As seen in Sec. IV, the theory is quite successful in its predictions of the properties of the free surface of liquid argon. In the vicinity of a hard wall it predicts physically very reasonable oscillatory behavior. As discussed in Sec. II, the theory is clear and concise regarding the state-

ments of the approximations on which it is based. From this point of view it is visibly superior to its predecessors. The approximations involve an expansion of $F[n]$ in terms of density differences, the choice of the average density \bar{n} in the kernel [see Eqs. (2.3)–(2.5)], and the choice of the PY theory as that uniform-system theory from which the DF theory proceeds.

Of three approximations made, that involving the choice of \bar{n} is the only one for which we have made detailed checks. We have found the results to be insensitive to the choice of \bar{n} , provided that \bar{n} is chosen in a physically reasonable way (see Sec. IV). It is in principle possible to eliminate the need for such a choice. The basic PY equation (3.1), written in the form

$$c(\vec{r}, \vec{r}') = g(\vec{r}, \vec{r}') (1 - e^{\beta v(\vec{r} - \vec{r}')}), \quad (6.1)$$

together with a generalized version of (3.3),

$$g(\vec{r}, \vec{r}') - 1 = c(\vec{r}, \vec{r}') + \int d^3 r'' [g(\vec{r}, \vec{r}'') - 1] \times n(\vec{r}'') c(\vec{r}'', \vec{r}') \quad (6.2)$$

in principle yield $c(\vec{r}, \vec{r}')$, given $n(\vec{r})$. One could use our DF theory, together with this PY theory, for nonuniform systems to self-consistently determine both $n(\vec{r})$ and $c(\vec{r}, \vec{r}')$. This procedure removes the somewhat artificial construct \bar{n} from the formalism. The practicality of this approach is under investigation.

An even better theory would be one which utilized (6.1) and (6.2) together with an exact theory of $F[n]$ formulated in terms of densities and direct correlation functions. This theory would eliminate the expansion in density differences, leaving the Percus-Yevick equation as the single approximation in the theory. For the special case of the planar free surface this has been done by Triezenberg and Zwanzig³³ and Lovett *et al.*³⁴ Their approach requires that the geometry be such that the use of a continuous wave number is appropriate. For more general situations, e.g., small droplets, this is not the case. However, for the general case, it appears possible to achieve the stated goal using functional techniques developed by Lebowitz and Percus.³⁵ We hope to deal with this topic in a future publication.

*Work partially supported by NSF Grant Nos. DMR75-21866 and No. GH-33746.

¹N. D. Lang, in *Solid State Physics*, edited by H. Ehrenreich, F. Seitz, and D. Turnbull (Academic, New York, 1973), Vol. 28, p. 255.

²C. A. Croxton, *Adv. Phys.* **22**, 385 (1973).

³See, e.g., the article by C. B. Duke, in *Advances in Chemical Physics*, Vol. XXVII, edited by I. Prigogine and S. A. Rice (Wiley, New York, 1974), p. 1.

⁴C. Ebner and W. F. Saam, *Phys. Rev. B* **12**, 923 (1975); see also W. F. Saam and C. Ebner, *Phys. Rev. Lett.* **34**, 253 (1975).

- ⁵In the unstable portion of the two-phase region the PY solutions are unphysical and are not used. This point is further discussed in Sec. III.
- ⁶V. Bongiorno and H. T. Davis, *Phys. Rev. A* **12**, 2213 (1975).
- ⁷S. Toxvaerd, *J. Chem. Phys.* **55**, 3116 (1971).
- ⁸S. Toxvaerd, *Mol. Phys.* **26**, 91 (1973).
- ⁹See AIP document No. PAPS PLRAA-14-2264-39 for 39 pages of Percus-Yevick pair correlation functions for a Lennard-Jones (6-12) fluid. Order by PAPS number and journal reference from American Institute of Physics, Physics Auxiliary Publication Service, 335 East 45th St., New York, N. Y. 10017. The price is \$1.50 for each microfiche (98 pages), or \$5 for photocopies of up to 30 pages with \$0.15 for each additional page over 30 pages. Airmail additional. Make checks payable to the American Institute of Physics. This material also appears in *Current Physics Microfilm*, the monthly microfilm edition of the complete set of journals published by AIP, on the frames immediately following this journal article.
- ¹⁰J. K. Lee, J. A. Barker, and G. M. Pound, *J. Chem. Phys.* **60**, 1976 (1974); see also Ref. 11, which corrects an error in this work.
- ¹¹F. F. Abraham, D. E. Schreiber, and J. A. Barker, *J. Chem. Phys.* **62**, 1958 (1975).
- ¹²G. A. Chapela, G. Saville, and J. S. Rowlinson, *Discuss. Faraday Soc.* **59**, 22 (1975).
- ¹³K. S. Liu, *J. Chem. Phys.* **60**, 4226 (1974).
- ¹⁴J. Miyazaki, J. A. Barker, and G. M. Pound, *J. Chem. Phys.* **64**, 3364 (1976).
- ¹⁵P. Hohenberg and W. Kohn, *Phys. Rev.* **136**, B864 (1964).
- ¹⁶N. D. Mermin, *Phys. Rev.* **137**, A1441 (1964).
- ¹⁷This function is discussed by, e.g., A. L. Fetter and J. D. Walecka, *Quantum Theory of Many-Particle Systems* (McGraw-Hill, New York, 1971).
- ¹⁸An exception here is the simple analytic model presented in Sec. V.
- ¹⁹J. K. Percus and G. J. Yevick, *Phys. Rev.* **110**, 1 (1958).
- ²⁰See, e.g., C. A. Croxton, *Liquid State Physics-A Statistical Mechanical Introduction* (Cambridge U.P., Cambridge, England, 1973).
- ²¹J. DeBoer, J. M. J. Van Leeuwen, and J. Groeneveld, *Physica (Utr.)* **30**, 2265 (1964).
- ²²G. J. Throop and R. J. Bearman, *Physica (Utr.)* **32**, 1298 (1966).
- ²³A. A. Broyles, S. U. Chung, and H. L. Sahlin, *J. Chem. Phys.* **37**, 2452 (1962).
- ²⁴A. A. Khan, *Phys. Rev.* **134**, A367 (1964).
- ²⁵L. Verlet, *Physica (Utr.)* **30**, 95 (1964).
- ²⁶D. Levesque, *Physica (Utr.)* **32**, 1985 (1966).
- ²⁷R. O. Watts, *J. Chem. Phys.* **48**, 50 (1968); **50**, 984 (1969).
- ²⁸R. L. Kerber, *J. Chem. Phys.* **52**, 2436 (1970).
- ²⁹The experimental coexistence curve is that quoted by E. A. Guggenheim, *J. Chem. Phys.* **13**, 253 (1945), who cites the data of Onnes and Crommelin, *Comm. Phys. Lab. Univ. Leiden No. 131a* (1912).
- ³⁰See, e.g., T. Lukes and R. Jones, *J. Phys. A* **1**, 29 (1968).
- ³¹See, e.g., D. Stroud and N. W. Ashcroft, *Phys. Rev. B* **5**, 371 (1972), and references cited therein.
- ³²J. Rasaiah and G. Stell, *Mol. Phys.* **18**, 249 (1970).
- ³³D. G. Triezenberg and R. Zwanzig, *Phys. Rev. Lett.* **28**, 1183 (1972).
- ³⁴R. Lovett, P. W. Dehaven, J. J. Viecelli, Jr., and F. B. Buff, *J. Chem. Phys.* **58**, 1880 (1973).
- ³⁵J. L. Lebowitz and J. K. Percus, *J. Math. Phys.* **4**, 116 (1963).